International Immunology, Vol. 33, No. 2, pp. 79–90
doi:10.1093/intimm/dxaa060
Advance Access publication 5 September 2020

Bim establishes the B-cell repertoire from early to late in the immune response

Akiko Sugimoto-Ishige[1–3], Michishige Harada[2], Miho Tanaka[2], Tommy Terooatea[4], Yu Adachi[5], Yoshimasa Takahashi[5], Takashi Tanaka[3], Peter D. Burrows[6], Masaki Hikida[1] and **Toshitada Takemori[2,3]**

[1]Deparment of Life Science, Graduate School of Engineering Science, Akita University, Akita City, Akita 010-8502, Japan
[2]Drug Discovery Antibody Platform Unit,
[3]Laboratory for Inflammatory Regulation and
[4]Laboratory for Cellular Epigenomics, RIKEN Research Center for Integrative Medical Sciences, Kanagawa 230-0045, Japan
[5]Department of Immunology, National Institute of Infectious Diseases, Tokyo 162-8640, Japan
[6]Department of Microbiology, University of Alabama at Birmingham, Birmingham, AL 35294, USA

Correspondence to: T. Takemori; E-mail: toshitada.takemori@riken.jp or M. Hikida; E-mail: hikida@gipc.akita-u.ac.jp

Received 21 May 2020, *editorial decision* 31 August 2020; *accepted* 3 September 2020

Abstract

In T cell-dependent antibody responses, some of the activated B cells differentiate along extrafollicular pathways into low-affinity memory and plasma cells, whereas others are involved in subsequent germinal center (GC) formation in follicular pathways, in which somatic hypermutation and affinity maturation occur. The present study demonstrated that Bim, a proapoptotic BH3-only member of the Bcl-2 family, contributes to the establishment of the B-cell repertoire from early to late stages of immune responses to T cell-dependent antigens. Extrafollicular plasma cells grew in the spleen during the early immune response, but their numbers rapidly declined with the appearance of GC-derived progeny in wild-type mice. By contrast, conditional Bim deficiency in B cells resulted in expansion of extrafollicular IgG1$^+$ antibody-forming cells (AFCs) and this expansion was sustained during the late response, which hampered the formation of GC-derived high-affinity plasma cells in the spleen. Approximately 10% of AFCs in mutant mice contained mutated V_H genes; thus, Bim deficiency appears not to impede the selection of high-affinity AFC precursor cells. These results suggest that Bim contributes to the replacement of low-affinity antibody by high-affinity antibody as the immune response progresses.

Keywords: affinity selection, extrafollicular plasma cells, GC-dependent response, GC-independent response, niche

Introduction

In T cell-dependent antibody responses, B cells are activated by cognate T-cell interactions in the outer T-cell zone of secondary lymphoid organs and they then differentiate along either follicular or extrafollicular pathways, with a fraction of cells undergoing immunoglobulin (Ig) class switch recombination (1, 2). In the follicle, activated B cells form the germinal center (GC) following upregulation of the transcriptional repressor Bcl-6. GCs are generally considered as the sole sites of high-affinity plasma-cell or memory B-cell generation.

After cognate interactions with T cells, activated B cells in the extrafollicular pathways migrate to the splenic bridging channels or junction zones at the border between the T-cell zones and red pulp in the spleen (3). There they form foci of short-lived plasmablasts that produce relatively low-affinity antibodies encoded by germline V_H genes (4, 5). Thus, plasmablasts produce an early antibody response and play important roles in the initial defense against pathogens (6) and in the regulation of B-cell selection in the GC by modulating antigen accessibility, shielding antigens from access by lower-affinity B cells (7). Most of the plasmablasts are in S phase and the cell number typically peaks on day 4 after immunization before rapidly declining by day 7 (3, 8). However, the reason why these cells are rapidly lost remains elusive.

GC-dependent plasma cells, which improve the quality of antibody responses with the accumulation of somatic mutations in their V_H and V genes and affinity maturation, are generated after the appearance of the extrafollicular plasmablasts (9, 10). It has been proposed that most long-lived plasma cells arise from GCs (10, 11) and that their long-term survival depends on signals derived from their environment. During the early phase of the response, plasma cells migrate from the spleen and lymph nodes to the bone marrow (BM)

compartment (12). Antibody-forming cells (AFCs) appear in BM about day 10 and gradually accumulate during the late primary response (9, 13). Thus, the preferential accumulation of high-affinity AFCs in BM is a key element in the affinity maturation of serum antibody and is crucial for protective immunity.

Apoptotic cell death plays a critical role in the development and functioning of the immune system (14). In particular, the pro-apoptotic protein subgroup called 'BH3-only', which includes Bim, is critical in the initiation of apoptosis in response to many external stimuli. Bim interacts with specific subsets of anti-apoptotic BCL-2 family members, such as Mcl-1, Bcl-2, Bcl-xL and Bcl-w, yielding combinatorial signaling pathways that result in apoptosis (15).

B cell receptor (BCR) engagement promotes interaction of Bim with Bcl-2, inhibiting its survival activity, indicating that Bim is an important player in BCR-mediated apoptosis and in B lymphocyte deletion (16). It has been reported that germline Bim-deficient mice expanded the number of low-affinity IgG1$^+$ AFCs in the spleen and BM, which were detected late in the immune response (17). The loss of Bim in AFCs resulted in their long-life span *in vitro*, suggesting that they may persist for a long period of time *in vivo* after their generation. The lack of affinity maturation in AFCs detected in the late immune response was discussed in this report as being due to the possibility that Bim is critical for apoptosis of GC-derived AFCs, but this speculation was not experimentally verified.

As Bim proteins are expressed in a wide variety of tissues (18) and Bim germline deletion causes multiple immunological dysfunctions (19–23), it remains unclear whether the aberrant AFC response in germline Bim-deficient mice was a consequence of the intrinsic loss of Bim in B cells. To define the role of Bim in AFCs under more physiological conditions, we developed a mouse strain with a conditional *Bim* allele and crossed these mice with Cγ1- or mb-1-Cre transgenic strains (24, 25). We found that conditional Bim deficiency resulted in expansion of low-affinity AFCs in spleen prior to GC formation, which limited the recruitment of GC progeny during the late phase of the immune response. However, selection of the high-affinity GC B cells was comparable in Bim-deficient mice and Bim-sufficient mice, suggesting that Bim is not critical for apoptosis of low-affinity GC-derived AFCs.

Methods

Mice and immunizations

Eight-weeks-old C57BL/6 female mice were purchased from Clea Japan Inc. mb1-cre, Cγ1-cre and Bcl6$^{f/f}$ mice have been described previously (26). Mice were immunized intraperitoneally with 100 μg 4-hydroxy-3-nitro phenylacetyl coupled with chicken-γ-globulin (NP_{15}-CGG) precipitated in alum (27) or, in some experiments, with 50 μg NP-Ficoll (Biosearch Technologies, Middlesex, UK) in phosphate-buffered saline (PBS) (26) or with 10 μg inactivated influenza virus (PR8), as described later. All experiments were performed in accordance with guidelines established by the RIKEN Animal Safety Committee.

Generation of Bim *conditional knockout mice*

Bim floxed mice carrying two loxP sites in the introns flanking exon 5 of the *Bim* gene (Supplementary Figure 1A) were generated as follows. To construct the targeting vector, we amplified the genomic DNA fragments of long-arm (LA) and short-arm (SA) region of the *Bim* gene (Supplementary Figure 1A) from the C57BL/6 embryonic stem (ES) cell line Bruce4 (28) by PCR and subcloned them into a pEZ-Frt-Lox-DT vector. Similarly, the targeting region was subcloned into another pEZ-Frt-Lox-DT vector. The targeting region containing the loxP sequence was amplified and inserted between the LA and SA of the targeting vector. The targeting construct was linearized and electroporated into Bruce4 ES cells. Cells were expanded with G418 and resistant clones were screened by PCR and Southern blot analysis. An established ES clone was injected into blastocysts from BALB/c mice to produce chimeric mice. After obtaining germline transmission, the resultant mice were crossed with FLPe-expressing deleter mice (29) to remove the FRT-franked Neo cassette (Supplementary Figure 1A). Obtained Bim$^{f/+}$ mice were crossed to C57BL/6 mice, *mb1*-cre mice or *Cγ1*-cre mice. To establish Bcl6 and Bim double conditional knockout (KO) mice, we first generated Bim$^{f/f}$; Bcl6$^{f/f}$ mice and Bim$^{f/+}$; Bcl6$^{f/+}$; mb1-cre$^{+/-}$ mice by crossing Bim$^{f/f}$; mb1-cre$^{+/-}$ and Bcl6$^{f/f}$; mb1-cre$^{+/-}$ mice. Thereafter, Bim$^{f/f}$; Bcl6$^{f/f}$ and Bim$^{f/+}$; Bcl6$^{f/+}$; mb1-cre$^{+/-}$ mice were crossed to establish Bim$^{f/f}$; Bcl6$^{f/f}$; mb1-cre$^{+/-}$ double conditional KO mice. All the strains were confirmed to carry the *Bim* and *Bcl6* floxed alleles before crossing with other strains.

Flow cytometric analysis of naive mice

This was performed as previously described (26). In brief, to prepare single-cell suspensions, spleens, Peyer's patches (PPs) and BM were minced. Splenocytes and BM cells were depleted of red blood cells, followed by incubation with a blocking FcγRII/III monoclonal antibody (mAb) (2.4G2; American Type Culture Collection, Manassas, VA, USA).

For analysis of BM B cells in unimmunized mice, the cells were incubated with biotinylated mAbs against CD3, CD90.2, TER119, Gr-1, CD11b, DX5 and NK1.1 (all purchased from BioLegend, San Diego, CA, USA), followed by staining with anti-B220^{BV510} (BioLegend), anti-IgM$^{Pacific\ blue}$ [conjugated in our laboratory using a Molecular Probe labeling kit (Thermo Fisher Scientific, Waltham, MA, USA)], anti-AA4.1^{APC} (BioLegend), anti-CD24^{FITC} (BioLegend), anti-CD43^{PE} (BD Bioscience, San Jose, CA, USA) and streptavidin$^{PE\text{-}CF594}$ (BD Bioscience). BM B220$^+$ cells were separated into AA4.1$^+$ and AA4.1$^-$ cells, immature and mature B cell populations, respectively (30). The frequency of pre–pro-B cells (CD24^{low}CD43^{hi}), pro-B cells (CD24^{int}CD43^{int}) and pre-B cells (CD24^{hi}CD43^{lo}) was analyzed in the AA4.1$^+$B220$^+$ population (31).

For analysis of B cells in the spleen, splenocytes from unimmunized mice were incubated with a mixture of biotinylated mAbs against CD138 (BD Bioscience), CD43 (BD Bioscience), CD3, CD90.2, TER119, Gr-1, DX5 and NK1.1, followed by staining with B220^{BV510} (BioLegend), CD21^{FITC} (BD Bioscience), AA4.1^{APC}, IgM^{PacificBlue} and streptavidin$^{PE\text{-}CF594}$ (BD Bioscience). B220$^+$AA4.1$^-$ cells were separated into FO (IgM^{int}CD21^{int}) and MZ (IgM^{high}CD21^{high}) B cells. B220$^+$AA4.1$^+$

B cells were separated into Transitional-1 (T1, IgM^{high}CD23^{dull}), T2 (IgM^{high}CD23^{high}) and T3 (IgM^{dull}CD23^{dull}) B cells.

For the analysis of CD4 and CD8 T cells in the spleen, splenocytes from unimmunized mice were incubated with a mixture of mAbs against CD4^{APC} (BioLegend), TCRβ^{PE} (Thermo Fisher Scientific), CD8α^{FITC} (BioLegend) and B220^{BV510} (BioLegend).

For the analysis of B cells in PPs, cells were incubated with anti-CXCR5^{APC} (BD Bioscience) at 37°C for 30 min. After washing, cells were stained with anti-Fas$^{PE\text{-}Cy7}$ (BD Bioscience), anti-PD-1^{PE} (Thermo Fisher Scientific), anti-CD4^{BV421} (BioLegend) and Peanut Agglutinin (PNA)^{FITC} (Vector Laboratories, Burlingame, CA, USA).

After washing, cells were re-suspended in a staining buffer containing 1 μg/ml propidium iodide (PI) and analyzed using a FACSAria II or III (BD Bioscience) or a BD LSRFortessa X-20. To improve the accuracy of lymphocyte subset analysis, only cells exhibiting forward and large-angle scatter typical of lymphocytes (the lymphocyte gate; eliminating monocytes and granulocytes) were analyzed (27). For all experiments reported here, only cells negative for PI and streptavidin$^{PE\text{-}CF594}$ staining were gated for further analysis. More than 100 000 total events were collected for each file and then analyzed using FlowJo software (BD Bioscience).

Cell purification and analysis of immunized mice

Spleens from NP-CGG immunized Bim$^{+/+}$ or Bim$^{f/f}$ mice heterozygous for mb1-cre were minced and incubated with collagenase IV (200 unit/ml; Merck, Darmstadt, Germany) and DNase I (20 μg/ml; Roche, Basel, Switzerland) for 30 min at 37°C, before depletion of red blood cells.

For single-cell sorting of major histocompatibility complex class II (MHC II) and CD83-labeled cells for V_H sequence analysis, cells were incubated with a mixture of biotinylated mAbs against IgM (Thermo Fisher Scientific), IgD, CD3, CD90.2, TER119, Gr-1, F4/80, DX5, AA4.1 (Thermo Fisher Scientific), NK1.1, CD43, CD11b and CD11c (BioLegend), followed by incubation with streptavidin microbeads (Miltenyi Biotec, Bergisch Gladbach, Germany). Thereafter, the cells negatively selected by the MACS system (Miltenyi Biotec) were stained with anti-CD83^{PE} (BioLegend), anti-I-A/I-E$^{Alexa\ Fluor700}$ (MHCII$^{Alexa\ Fluor700}$, BioLegend), anti-CD38^{BV510} (BD Bioscience), anti-IgG1^{BV421} (BD Bioscience), NIP-BSA^{APC}, anti-Fas^{FITC} (BD Bioscience), streptavidin$^{PE\text{-}CF594}$, followed by FACS single-cell sorting to purify CD83^{high}/MHCII^{high}, CD83^{negative}/MHCII^{high} and MHCII^{dull} GC subsets.

For single sorting of AFCs, splenocytes from NP-CGG immunized mice were incubated with 2.4G2, followed by staining with a mixture of FITC-conjugated mAbs against anti-IgM (Thermo Fisher Scientific), anti-IgD (Thermo Fisher Scientific), anti-CD11b (BioLegend), anti-CD90.2 (BioLegend), anti-Gr-1 (BioLegend), anti-DX5 (BioLegend) and anti-TER119 (BioLegend). After washing, cells were incubated with anti-FITC microbeads (Miltenyi Biotec), followed by negative selection using the MACS system. Thereafter, cells were stained with biotinylated anti-Igλ$_{1,2,3}$ (BD Bioscience). After washing, cells were stained with anti-CD138^{PE} (BD Bioscience), anti-B220^{BV510} (BioLegend), NIP-BSA^{APC} and streptavidin^{BV421} (BD Bioscience). Single AFCs were sorted from the FITC^{negative}/Igλ^{+}/CD138^{high}/NIP^{+}/B220^{dull} population. All single-cell sorting was performed on a FACSAria III (BD Bioscience).

Virus and vaccine preparation

The PR8 (H1N1) influenza virus was propagated in embryonated chicken eggs and purified through a 10–50% sucrose gradient as previously described (32). To produce split vaccines, purified live viruses were suspended in 0.1% Tween 80 and mixed with an equal volume of ether. After vortexing, the mixture was centrifuged to separate the aqueous and ether phases and the ether phase was discarded. After several rounds of extraction, the remaining aqueous phase was collected and then treated with formalin at 4°C for 1 week before use.

Tissue immunofluorescence assay

Tissue immunofluorescence assay was performed as previously described (33). Briefly, spleens were obtained from mice 12 days after immunization with NP-CGG. Spleens were embedded in O.C.T. compound (Miles, Elkhart, IN, USA), frozen in a dry ice/ethanol bath for 30 s and stored at –80°C. Frozen sections (7 μm thick) were fixed in acetone on ice for 10 min. After washing with staining buffer (0.1 M Tris–HCl, pH 8.0, 0.1 M NaCl, 0.1% Tween 20, 1% BSA), the sections were pre-incubated with staining buffer containing 2.4G2 (100 μg/ml) and 10% heat-inactivated normal goat serum for 4 h at room temperature or overnight at 4°C. All reagents for staining were centrifuged at 15 000 r.p.m. for 20 min before use. To mark GCs in tissues, the sections were stained with a mixture of anti-GL7$^{Alexa\ Fluor\ 488}$ (BioLegend), anti-CD38^{APC} (Thermo Fisher Scientific) and anti-mouse IgG1^{BV421} (BD Biosciences). The samples were examined by fluorescence microscope (BZ-X700; KEYENCE, Osaka, Japan). Figure 3 shows representative images from samples of three mice.

Sequence analysis of the heavy chain variable region of NP-specific B cells

The sequence analysis was carried out as previously described (26). In brief, single cells were sorted directly into 96-well PCR plates containing 10 μl of 5 ng/μl carrier RNA (QIAGEN, Hilden, Germany) as described in the *Cell purification and analysis of immunized mice* section and immediately frozen. After thawing, RT–PCR was performed with SuperScript One-Step High Fidelity (Thermo Fisher Scientific) using primer pairs consisting of V186.2 sense (5′-TTCTTGGCAGCAACAGCTACA-3′) and Cγ1 external anti-sense (5′-GGATCCAGAGTTCCAGGTCACT-3′) according to the manufacturer's instructions (25-μl final volume). Next, using 1 μl of the first RT–PCR product as template, a second round of PCR was performed using primer pairs consisting of V186.2 sense and Cγ1 internal anti-sense (5′-GGAGTTAGTTTGGGCAGCAG-3′) and Platinum Pfx DNA polymerase (Thermo Fisher Scientific). The purified PCR products were then directly sequenced using Cγ1 internal anti-sense primers. Expression of Blimp-1 (*Prdm1*) mRNA was also confirmed in single AFC as follows; a primer set (Blimp-1 external forward primer: 5′-TTCAAGCCGAGGCATCCTT, and Blimp-1 reverse

primer: 5′-AGTGTAGACTTCACCGATGAGG-3′) was added to the first round RT–PCR reactions for V186.2-Cγ1 amplification. Next, using 1 μl of the first RT–PCR product as template, a second round of PCR was performed using primer pairs Blimp-1 forward internal primer: 5′-GAACCTG CTTTTCAAGTATGCTG-3′ and Blimp-1 reverse primer. The second PCR products were subjected to agarose gel electrophoresis and EtBr staining for semi-quantitative analysis of Blimp-1 expression.

ELISPOT assay

ELISPOT assays were performed based on previously described methods (26, 27). Briefly, pre-wetted MultiScreen HTS-IP 96 well plates (Merck) were coated with NP_2-BSA or NP_{18}-BSA at RT for 2 h. After PBS washing, wells were blocked with PBS containing 1% BSA (BSA/PBS). Splenocytes from Bim-deficient mice (2×10^4/well) and Bim-sufficient mice (1×10^5/well) and BM cells (2×10^5/well) were plated into each well, and the plates were incubated at 37°C, 5% CO_2 for 2–3 h. Plates were washed with PBS containing 0.1% Tween 20 (PBST), followed by overnight blocking with BSA/PBS. Next day, plates were incubated with alkaline phosphatase anti-mouse IgG1 (Southern Biotech, Birmingham, AL, USA), followed by washing with PBST buffered to pH 8.5 with 0.1 M Tris–HCl and development as previously described (27). Spots on the wells were counted under a stereo microscope.

ELISA assays

ELISA assays were performed as previously described (26). The amount of serum anti-NP IgG3 or IgM antibodies from NP-Ficoll immunized mice was calculated based on an anti-NP IgG1 mAb as a standard and described in arbitrary units (arb. unit). For detection of serum anti-HA IgG antibodies, 2 μg/ml inactivated flu virus (PR8) was coated as antigen. The amount of anti-HA IgG antibodies was calculated based on a standard curve generated with a control serum containing anti-PR8 IgG, which was generated by Y.A. and Y.T.

Statistical analysis

Student's *t*-test and the Mann–Whitney non-parametric (two-tailed) test were used with KaleidaGraph 4.5 software (Synergy Software, Pennsylvania, USA) or Microsoft Excel software (Microsoft, Washington, DC, USA). $P < 0.05$ was considered to indicate a significant difference.

Results

Bim does not regulate the T cell-independent response

We established mutant mice carrying a loxP-flanked *Bim* exon 5 allele ($Bim^{f/f}$), the exon encoding the BH3 domain (Supplementary Figure 1A and B), which is critical for Bim function [reviewed by Sionov *et al.* and Bouillet *et al.* (34, 35)]. Thus, a mutant Bim protein lacking the BH3 domain does not interact with anti-apoptotic Bcl-2, Bcl-xL or Bcl-w (36), resulting in the complete loss of the ability of Bim to induce apoptosis. To investigate the B-cell development in unimmunized mice, $Bim^{f/f}$ mice were crossed with mice in which a Cre cDNA was knocked-in into the *mb-1* locus [mb-1-cre; (25)]. Since mb-1 (Igα or CD79A) is expressed beginning at the early pro-B cell stage, *Bim* should be deleted in all B lineage cells.

Previous studies suggested that Bim proteins are expressed in pro-B pre-B, immature B and mature B cells (37) and that conditional loss of *Bim* exon 2–4 (Mb1-$Cre^{ki/+}$$Bim^{fl/fl}$) led to approximately 2-fold higher numbers of mature B cells in the spleen than observed in control mice (38). Likewise, the conditional deletion of *Bim* exon 5, which includes the BH3 domain, in B cells resulted in a small, but statistically significant increase in cell numbers in the spleen (Fig. 1A). It did not affect overall cellularity of BM or PPs (Fig. 1A), except for a marginal reduction in pre-B cells (Fig. 1B), or the numbers of B cells or T cells in the spleen (Fig. 1C and D). We hypothesized that reduction in number of pre-B cells in Bim-deficient mice may reflect Bim activity for promoting cell cycle progression, which was observed in an *in vitro* analysis (39). However, Bim deficiency resulted in a significant increase in GC B cell numbers in PPs (Fig. 1E), which may probably reflect a role of Bim in selection of pre-GC B cells, as proposed based on results from an *in vitro* culture system (40).

To examine whether conditional *Bim* deletion affects B cell immune responses, $Bim^{f/f}$;mb-1-$cre^{+/-}$ mice were immunized with the hapten NP-Ficoll. The levels of total and high-affinity IgG3 and IgM anti-NP antibodies were mostly comparable in Bim-sufficient ($Bim^{+/+}$;mb-1-$cre^{+/-}$) and Bim-deficient ($Bim^{f/f}$;mb-1-$cre^{+/-}$) mice, suggesting that Bim is not involved in the T cell-independent B cell response (Fig. 2A and B).

Bim deletion in B cells results in enhanced antibody production to T cell-dependent antigens

To examine whether Bim affected T cell-dependent B-cell immune responses, Bim-deficient mice were immunized with NP coupled with chicken gamma globulin (CGG). Consistent with a previous report (17), the level of IgG1 anti-NP antibody was significantly enhanced in Bim-deficient mice compared with Bim-sufficient mice (Fig. 2C). The average affinity of NP-specific day 14 serum antibody in the same mice was estimated by ELISA and neither Bim-deficient nor Bim-sufficient mice contained significant levels of the high-affinity component at this time point (Fig. 2D). Increased levels of IgG1 antibodies in Bim-deficient mice were also observed in response to influenza virus immunization, although the differences did not reach statistical significance at day 10 after immunization, owing to a low level of antigen-specific serum antibodies in one of the KO mice (Fig. 2E). As shown in Fig. 2F, the results in mice in which *Bim* was deleted by mb1-$cre^{+/-}$ were reproduced in $Bim^{f/f}$; γ1-$Cre^{+/-}$ mutant mice (24), in which the level of IgG1 anti-NP serum antibodies was increased up to day 40 after immunization. As shown in Fig. 2G, the ratio of NP_2/NP_{18} was reduced in KO mice (8.5, 8.7, 12.0, 12.6) at day 40 after immunization compared with control mice (13.6, 19.0, 21.9, 29.8), except for one mouse which had a ratio of 6.9. Although the differences did not reach statistical significance, these observations, along with the significantly decreased production of NP-specific high-affinity AFC in KO mice, collectively suggest an impairment in antibody affinity maturation in Bim-deficient mice (see Fig. 3).

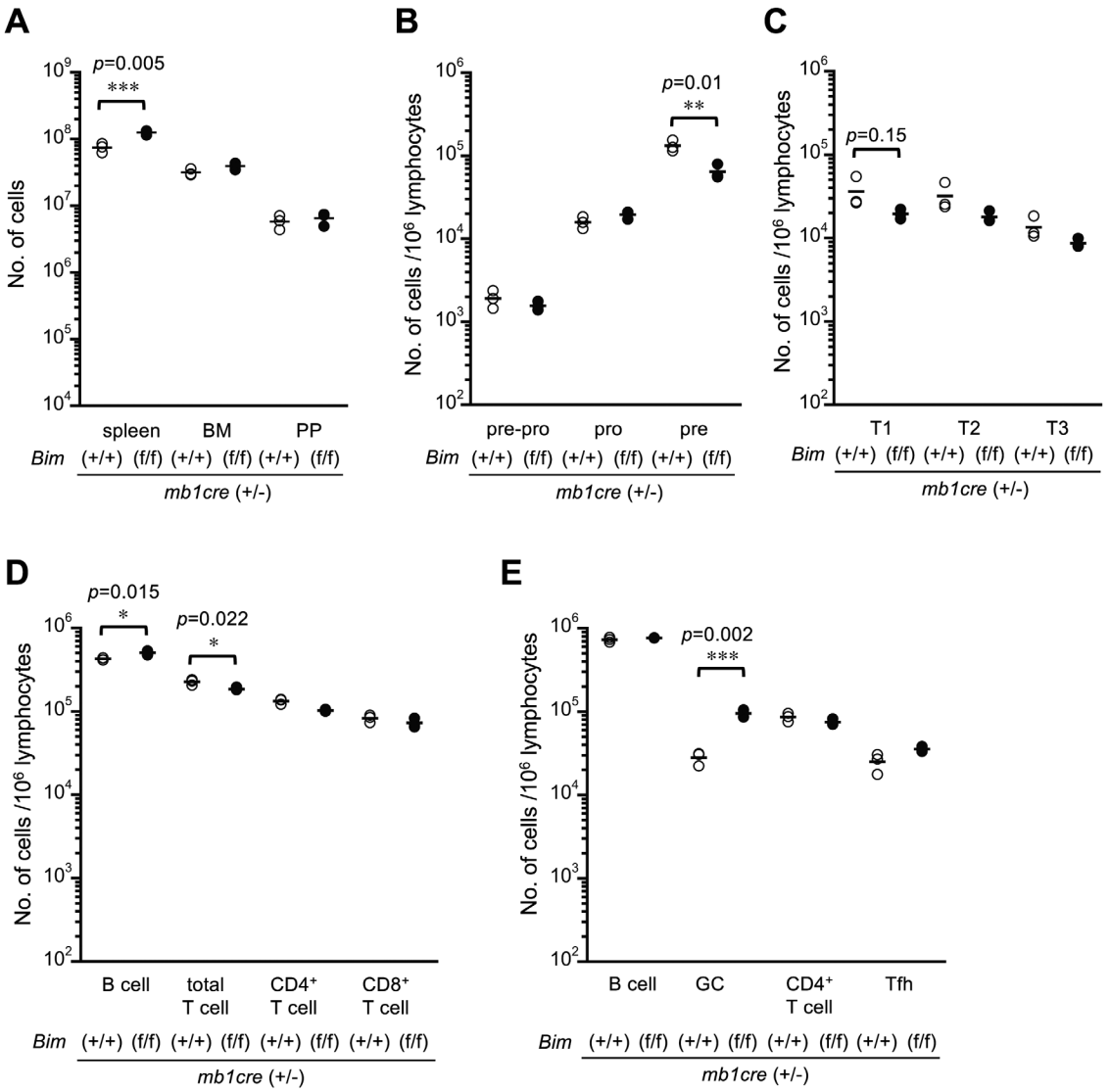

Fig. 1. Frequency of lymphoid cells in BM, spleen and PPs in Bim-deficient and Bim-sufficient mice. B and T cell numbers in non-immunized Bim-sufficient (open circles) and Bim-deficient (closed circles) mice. Genotypes are indicated at the bottom of each graph. (A) nucleated cells in spleen, BM and PPs, (B) bone marrow B cells in the pre-pro-, pro- and pre-B stages, (C) immature transitional B cells (T1, T2, T3 subsets) in spleen, (D) B and T cells in the spleen, (E) B cells, PNA⁺ GC B cells, CD4⁺ T cells and Tfh cells in PPs. In (B), (C), (D) and (E), cell numbers per 1×10^6 cells within the lymphocyte gate are shown (see Methods). $^*P < 0.05$, $^{**}P < 0.01$ and $^{***}P < 0.005$.

As shown in Fig. 3A and B, ELISPOT analysis suggested that Bim deficiency ($Bim^{f/f}$;mb-1-$cre^{+/-}$) resulted in 100- and 10-fold increases in the numbers of IgG1⁺ AFCs in the spleen (Fig. 3A) and BM (Fig. 3B), respectively, compared with control mice ($Bim^{+/+}$;mb-1-$cre^{+/-}$). However, the number of AFCs in BM was much lower than in spleen in both mouse strains. The proportion of the high-affinity compartment of AFCs was clearly higher in the spleen and BM of Bim-sufficient than in Bim-deficient mice (Fig. 3C). Consistent with the results in Fig. 3A, immunohistochemical analysis illustrated that a large number of cells with high levels of IgG1 antibodies in the cytoplasm filled the red pulp of the spleen in Bim-deficient mice at 12 days after immunization (Fig. 3D, top panel), whereas only a small number of such cells were found in extrafollicular foci located at the junction of the T-cell zone and red pulp of the spleen in control mice (Fig. 3D, lower panel).

Together, these results suggest that conditional Bim deficiency in B cells resulted in enhanced T cell-dependent IgG1 antibody responses but had no demonstrable effect on T cell-independent antibody responses.

Bim regulates the generation of AFCs in the early immune response to a T cell-dependent antigen

The anti-NP response in C57BL/6 mice is dominated by λ light chain-bearing antibodies in which the V_H domain is encoded by a re-arranged V186.2 V gene segment (41). As shown in Fig. 4A and Table 1, there was a clear difference in both the frequency and distribution of mutations in V186.2 genes

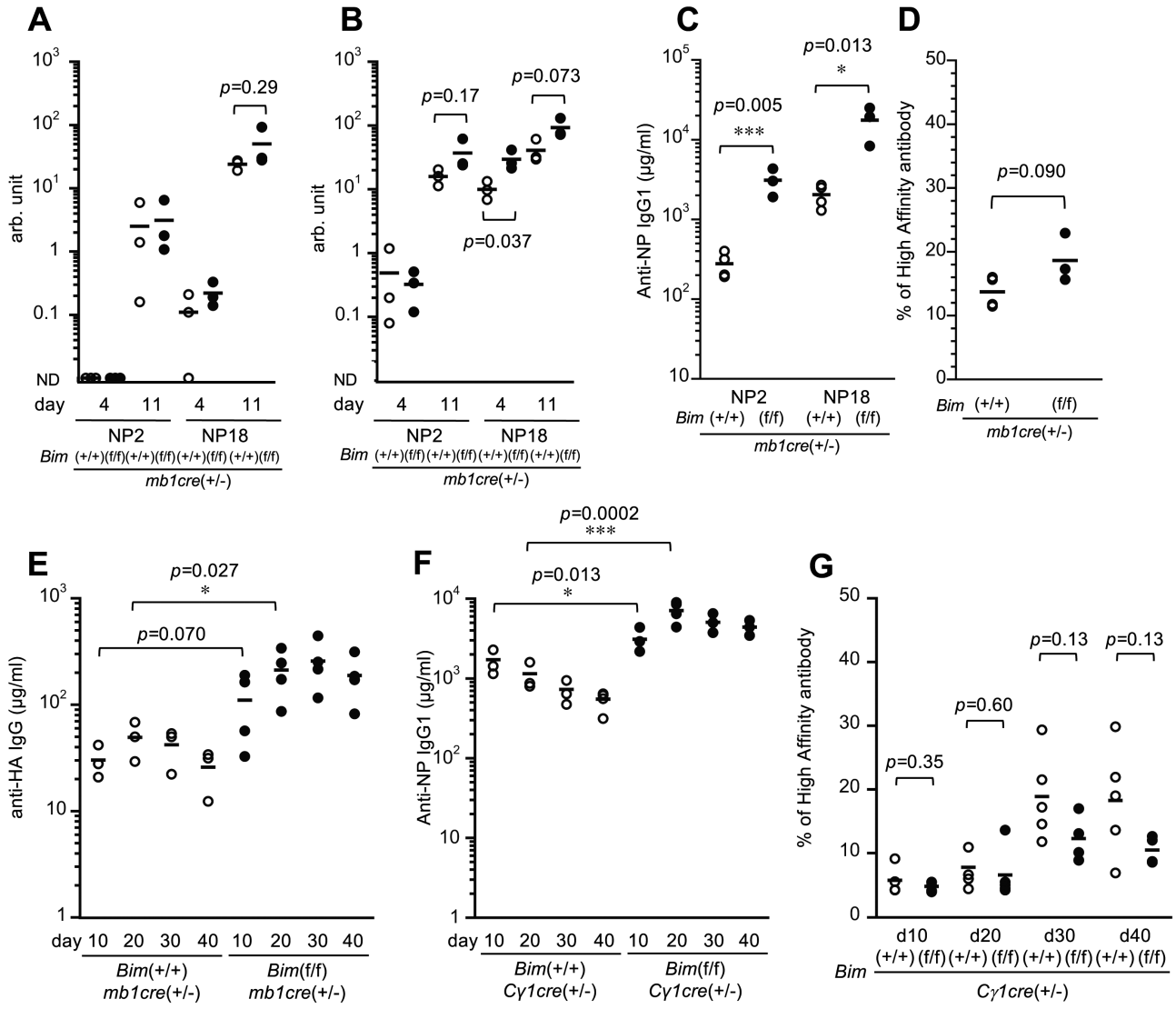

Fig. 2. Bim deficiency results in enhanced antibody production in response to T cell-dependent antigens, but not to T cell-independent antigens. (A and B) The levels of serum anti-NP IgG3 (A) and IgM (B) antibodies in Bim-sufficient (open circles) and Bim-deficient (closed circles) mice at day 4 and 11 after immunization with NP-Ficoll. The levels of total NP_{18}-binding (NP18) and high-affinity NP_2-binding (NP2) anti-NP IgG3 or IgM antibodies in the serum were measured by ELISA. Levels of the serum immunoglobulins were quantified against a purified standard anti-NP IgG1 mAb that was also included in the assays and expressed as arbitrary units, calculated as the serum dilution corresponding to 50% antigen binding/standard antibody dilution given 50% antigen binding. Each circle represents the result from an individual mouse. (C) Bim-sufficient (open circles, $n = 4$) and Bim-deficient (closed circles, $n = 3$) mice were immunized with NP-CGG in alum. After 2 weeks, total (NP18) and high-affinity (NP2) anti-NP IgG1 antibodies in the serum were measured as described in (B). Each circle represents the result from an individual mouse. (D) The concentrations of NP_2-binding and NP_{18}-binding IgG1 antibodies were determined by ELISA, and affinity maturation was calculated as the ratio of NP_2/NP_{18} IgG1 antibody. Data from Bim-sufficient (open circles) and Bim-deficient (closed circles) mice are indicated. Each circle represents the result from an individual mouse. (E) Bim deficiency resulted in enhanced anti-influenza virus antibody responses. Bim-sufficient (open circles, $n = 3$) and Bim-deficient (closed circles, $n = 4$) mice were immunized with inactivated influenza virus PR8 in AddaVax™. Immune sera were collected from individual mice at indicated times after the immunization and anti-hemagglutinin (HA) IgG1 antibodies in serum were measured by ELISA. (F) Bim-sufficient (open circles, $n = 5$) and Bim-deficient (closed circles, $n = 4$) mice (Cγ1-cre) were immunized with NP-CGG in alum. Immune sera were collected from individual mice at the indicated time after immunization and the levels of serum anti-NP IgG1 antibodies were measured by ELISA. Experiments were performed three times. (G) The concentrations of NP_2-binding and NP_{18}-binding IgG1 antibodies from Bim-sufficient (open circles) and Bim-deficient (closed circles) mice were determined by ELISA as described in (F) and the ratios of NP_2-binding versus NP_{18}-binding IgG1 antibody were plotted. Each circle represents the result from an individual mouse. $^*P < 0.05$, $^{**}P < 0.01$ and $^{***}P < 0.005$.

between Bim-deficient and control mice at day 14 after immunization, whereas similar junctional diversity was noted in both strains (Supplementary Figure 2A and B). Most strikingly, an unusually large percentage of sequences from *Bim*$^{-/-}$ AFCs had zero mutations (86%), compared with approximately 14% of those from control mice. Accordingly, the average number of mutations per V_H186.2 gene sequence was 2.7 in *Bim*$^{+/+}$ B cells versus only 1.5 in *Bim*$^{-/-}$ B cells (Table 1). These results

suggest that non-mutated IgG1 AFCs were expanded and sustained in the spleen in Bim KO mice, whereas these cells were mostly replaced by GC-derived AFCs in control mice.

In normal AFCs, an affinity-enhancing mutation involving the replacement of tryptophan with leucine was dominantly selected in CDR1 at position 33 in the V_H186.2 gene containing Tyr at the border of the D segment (W33L/Tyr95) (64% per mutated V_H gene, see Table 1). The low frequency of overall mutations coupled with the high incidence of the single affinity-enhancing mutation (W33L) in the V_H genes of AFCs in control mice suggests that the high-affinity cells are selected in the early GC response. We performed a genealogical analysis of V_H186.2 clonal families of AFCs in Bim-sufficient mice as previously described (42) and observed that clones rapidly acquired affinity maturation through W33L replacement, followed by accumulation of other replacement mutations, providing diversification within the family by day 14 after immunization. On the other hand, clones without the W33L replacement continued to accumulate numerous mutations (Supplementary Figure 3), which may in combination provide an equivalent increase in affinity as previously postulated (41).

As shown in Fig. 4A and Table 1, the ratio of the high-affinity (W33L) to mutated V_H genes in Bim-deficient mice was half of that in control mice, supporting the idea that loss of *Bim* does not prevent the process of somatic hypermutation in GCs during the process of AFC differentiation.

Table 1. Summary of VH gene mutation in AFC[a]

Bim	Mutated VH gene[b]	Number of mutations[c]	W33L/Tyr95		K58R/Gly95[f]
			Total[d]	Mutated[e]	
+/+	58/65	155/58	37/65	37/58	<1/65
	89.2%	2.7	56.9%	63.8%	
–/–	10/70	15/10	3/70	3/10	<1/70
	14.3%	1.5	4.3%	30.0%	

[a]Data are based on the sequence analysis of *VH186.2* genes (Fig. 4A).
[b]% was calculated as 100 × (number of mutated V_H genes/total number of *VH186.2* genes sequenced).
[c]Number of mutations/total number of V_H genes sequenced.
[d]% was calculated as 100 × (number of V_H genes with W33L clonotype/total number of *VH186.2* genes sequenced).
[e]% was calculated as 100 × (number of V_H genes with W33L clonotype/number of mutated *VH186.2* genes).
[f]% was calculated as 100 × (number of V_H genes with K58R clonotype/total number of *VH186.2* genes sequenced).

Selection of high-affinity cells in both Bim-deficient and Bim-sufficient mice

To learn whether selection for high-affinity antibodies was properly processed in the GCs of Bim-deficient mice, we analyzed the accumulation of mutations in the V_H genes of both control and mutant mice at 14 days after immunization.

CD83 has been used as a marker for light zone (LZ) B cells during the GC reaction (43) and CD83 expression in centrocytes helps to stabilize MHC II protein on the cell surface (44). We separated GC B cells into $CD83^{+}MHC\ II^{high}$, $CD83^{neg}MHC\ II^{high}$ and $CD83^{neg}MHC\ II^{dull}$ subsets (Fig. 4B) under the assumption that the $CD83^{+}MHC\ II^{high}$ GC B-cell population would be enriched in the LZ, where B-cell affinity selection occurs. As shown in Fig. 4B and Table 2, the frequency of mutated V_H genes was comparable in the three subsets of mutant and control mice. The frequency of W33L high-affinity mutations in mutated V_H genes appeared to be slightly higher in the GC populations from Bim-deficient mice than in those from Bim-sufficient mice, thereby excluding the possibility that Bim deficiency affects the selection of high-affinity clones

Table 2. Summary of V_H gene mutation in GC B cells[a]

Bim	Mutated V_H gene[b]	Number of mutations[c]	W33L/Tyr95		K58R/Gly95[f]
			Total[d]	Mutated[e]	
$CD83^{high}/MHC\ II^{high}$ GC B cells					
+/+	47/48	239/49	15/48	15/47	1/49
	(98%)	(4.9)	(31.3%)	(31.9%)	(2.0%)
–/–	39/41	166/41	21/41	21/39	1/41
	(95.1%)	(4.0)	(51.2%)	(53.8%)	(2.4%)
$CD83^{low}/MHC\ II^{low}$ GC B cells					
+/+	46/46	226/46	22/46	22/46	4/46
	(100%)	(4.9)	(47.8%)	(47.8%)	(8.7%)
–/–	39/39	186/39	27/39	27/39	1/39
	(100%)	(4.8)	(69.2%)	(69.2%)	(2.6%)
$CD83^{low}/MHC\ II^{high}$ GC B cells					
+/+	48/49	258/49	24/49	24/48	5/49
	(98.0%)	(5.3)	(49.0%)	(50.0%)	(10.2%)
–/–	37/38	166/38	21/38	21/37	1/38
	(97.4%)	(4.4)	(55.3%)	(56.8%)	(2.6%)

[a]Data are based on the sequence analysis of *VH186.2* genes (Fig. 4B).
[b]% was calculated as 100 × (number of mutated V_H genes/total number of *VH186.2* genes sequenced).
[c]Number of mutations/total number of V_H genes sequenced.
[d]% was calculated as 100 × (number of V_H genes with W33L clonotype/total number of *VH186.2* genes sequenced).
[e]% was calculated as 100 × (number of V_H genes with W33L clonotype/number of mutated *VH186.2* genes).
[f]% was calculated as 100 × (number of V_H genes with K58R clonotype/total number of *VH186.2* genes sequenced).

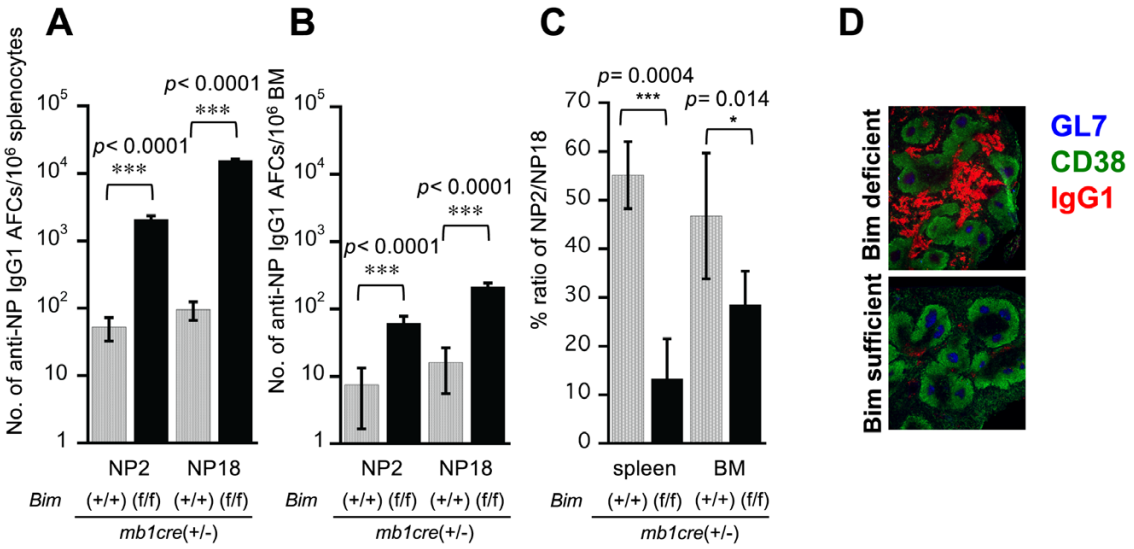

Fig. 3. Enhancement of low-affinity AFC generation in Bim-deficient mice in response to NP-CGG. (A–C) The role of Bim in the generation of antigen-specific antibody-secreting cells. Bim-sufficient (gray column) and Bim-deficient (black column) mice were immunized with NP-CGG (n = 3 each). Two weeks after the immunization, splenocytes (spleen) and bone marrow (BM) cells were separated and subjected to ELISPOT analysis to enumerate NP-specific IgG1-forming cells (AFCs) in culture wells. The ordinate represents the number ± SD of positive cells recognizing NP_2-BSA (NP2) (high affinity) and NP_{18}-BSA (NP18) (low + high affinity) per 1×10^6 spleen (A) and BM (B) cells. Experiments were performed twice. (C) The average affinity of NP-binding IgG1 AFCs in the spleen and BM in Bim-sufficient (gray column) and Bim-deficient (black column) mice at day 14 after immunization. The frequencies of NP_2-binding and NP_{18}-binding IgG1 AFCs from BM were determined by ELISPOT as described in (A–B), and the ratios of NP_2-binding versus NP_{18}-binding AFCs were then plotted. (D) Immunohistochemical analysis of IgG1$^+$ cells in the spleen. Cryosections were prepared from the spleens of Bim-deficient (top panel) and Bim-sufficient (lower panel) mice (n = 3) at day 12 after immunization with NP-CGG/alum. Sections were stained with anti-GL-7$^{\text{Alexa Fluor 488}}$ (blue), anti-mIgG1$^{\text{BV421}}$ (red) and anti-CD38$^{\text{APC}}$ (green). $^*P < 0.05$, $^{**}P < 0.01$ and $^{***}P < 0.005$.

during the GC reaction, at least at day 14 after immunization. A nucleotide exchange from glycine to arginine at position 58 in the V_H gene with Gly at position 95 (K58R/Gly95) is reported to be responsible for affinity maturation (45, 46), and this clonotype was detected in all GC subpopulations, albeit not at a high frequency (Table 2).

Bim deficiency caused an unusual expansion of extrafollicular IgG1$^+$ AFCs

Antigen-activated B cells in T cell-dependent responses differentiate along either the extrafollicular pathway independent of the GC reaction or the follicular pathway accompanied by GC formation upon expression of Bcl6 (1, 2). To examine the possibility that a large number of low-affinity AFCs were generated in mutant mice (Bim$^{f/f}$; mb-1-cre$^{+/-}$) along the extrafollicular pathway that is independent of the subsequent GC reaction, we established *Bim*/*Bcl-6* double KO mice (Bcl-6$^{f/f}$;Bim$^{f/f}$; mb-1-cre$^{+/-}$) by crossing Bim$^{f/f}$; mb-1-cre$^{+/-}$ mice with BCl-6$^{f/f}$; mb-1-cre$^{+/-}$ mice, and then immunized the mice with NP-CGG. As shown in Fig. 5A and B, these mice generated anti-NP IgG1 antibodies at approximately 5- to 10-fold higher levels than either the conditional *Bcl-6* KO or control mice, suggesting that Bim deficiency caused an unusual expansion of extrafollicular AFCs independent of the GC reaction (see Discussion).

Discussion

It has been reported that memory cells and AFCs generated in the early phases of B-cell responses are short lived and express low-affinity antibodies, whereas GCs generate high-affinity, long-lived memory and plasma cells (11).

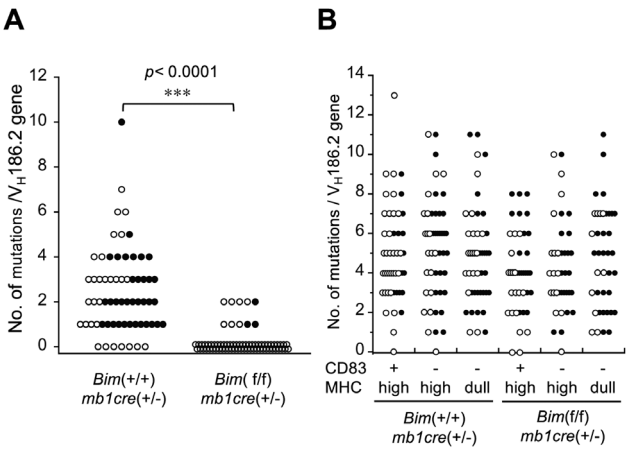

Fig. 4. V_H gene mutations in AFCs and GC B cells in Bim-deficient and -sufficient mice. (A) V_H186.2 gene mutations in NP-specific AFCs in mutant and control mice. Single NP-specific/IgG1$^+$ AFCs were purified from the pooled spleens of Bim-sufficient (+/+) (n = 5) and Bim-deficient (f/f) mice (n = 4) at day 14 after immunization and subjected to RT–PCR to amplify re-arranged *VH186.2-Cγ1* cDNA for sequencing (see Methods). Circles represent the number of mutations in individual clones. Closed circles represent W33L and K58R clones. (B) V_H186.2 gene mutations in NP-specific germinal center (GC) B cells in mutant and control mice. The GC B-cell population was separated into CD83^{high}/major histocompatibility complex class II (MHC II)^{high}, CD83^{negative}/(MHC II)^{high} and MHC II^{dull} subsets by FACS. Single NP-specific/IgG1$^+$ GC B cells in each population were purified from the pooled spleens of Bim-sufficient (+/+) (n = 6) and Bim-deficient (f/f) mice (n = 3) at day 14 after immunization and subjected to RT–PCR to amplify re-arranged *VH186.2-Cγ1* cDNA for sequencing. Circles represent the number of mutations in individual clones. Closed circles represent W33L and K58R clones. $^*P < 0.05$, $^{**}P < 0.01$ and $^{***}P < 0.005$.

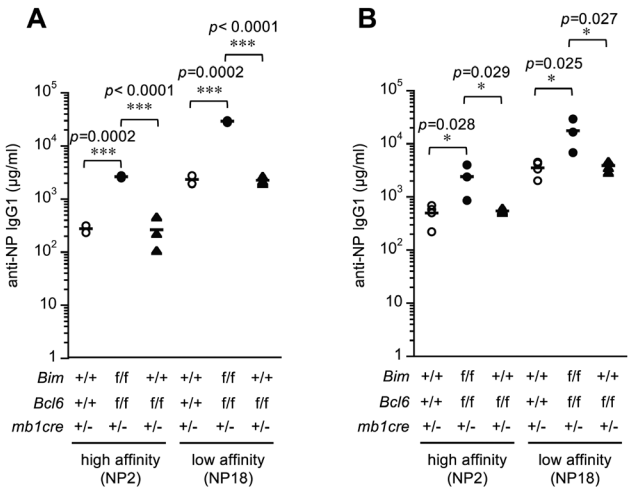

Fig. 5. Bim deficiency in Bcl-6 KO mice enhanced the generation of AFCs in the spleen. Conditional *Bim*/*Bcl-6* double KO (Bim$^{f/f}$Bcl-6$^{f/f}$; closed circles), *Bcl-6* KO (Bim$^{+/+}$Bcl-6$^{f/f}$; closed triangles) or control mice (Bim$^{+/+}$Bcl-6$^{+/+}$; open circles) were immunized with NP-CGG. After 2 weeks, immune serum was subjected to ELISA to estimate the levels of anti-NP IgG1 antibodies recognizing NP_2-BSA (NP2) (representing high-affinity antibody) and NP_{18}-BSA (NP18) (representing total antibody). Experiments were performed twice [experiment 1 (A) and experiment 2 (B) in right and left panels, respectively]. $^*P < 0.05$, $^{**}P < 0.01$ and $^{***}P < 0.005$.

The previous report suggested that germline deletion of *Bim* resulted in accumulation of IgG1$^+$ low-affinity AFCs in the spleen late in the immune response (17). However, the origin of these cells has remained unknown, e.g., whether they were generated from a GC response under an aberrant selection process without accumulation of high-affinity cells in the absence of Bim.

Consistent with the previous report, the present study showed that conditional B-cell Bim-deficient mice had increased levels of low-affinity antigen-specific IgG1 serum antibodies in response to NP-CGG, approximately 5–10 times above the levels found in Bim-sufficient mice. Consistently, the mutant mice showed a significant increase compared with control mice in the number of IgG1$^+$ AFCs in spleen and BM at 2 wks after immunization with NP-CGG. An increase in IgG1 antibodies in the *Bim*-deficient mice was also observed in response to inactivated influenza virus.

IgG1$^+$ AFCs in control mice had a high frequency of mutated V_H genes with the single affinity-enhancing Trp to Leu exchange, although these cells had fewer mutations in each V_H gene when compared with GC cells analyzed at the same time. The low frequency of mutations and high incidence of the single affinity-enhancing nucleotide exchange in the V_H genes of control AFCs compared with GC B cells indicates that the AFCs are an early selected product of the GC response, as previously reported (9).

We observed that selection of high-affinity V_H genes in GC B cells in response to NP-CGG occurred as efficiently in Bim-deficient mice as in Bim-sufficient mice. A minor population of Bim-deficient AFCs accumulated mutations in the V_H genes with high-affinity nucleotide exchanges at levels comparable to control AFCs, excluding the possibility that loss of Bim makes the exclusion of the low-affinity cells during AFC differentiation ineffective. These results support the notion that the large number of non-mutated IgG1$^+$ AFCs in Bim-deficient mice arose during the early immune response to a T cell-dependent antigen.

In fact, analysis of the anti-NP antibody response in conditional Bim/Bcl-6 double KO mice showed that Bim deficiency resulted in accumulation of a large number of low-affinity IgG1$^+$ AFCs in response to NP-CGG in mice deficient in GC formation. These results suggest that Bim-mediated apoptosis is required for the developmentally programmed death of extrafollicular plasmablasts in the early immune response.

It is generally accepted that plasma cell turnover involves competitive displacement of established plasma cells from their survival niches by newly formed plasma cells (47). Our immunohistochemical analysis suggested that large numbers of IgG1$^+$ AFCs filled the red pulp of the spleen in Bim-deficient mice at 2–4 weeks after immunization. The spleen, as well as BM, plays an important role in maintaining long-term humoral immunity (48), in which plasma cells may access relevant physical niches for survival (49). However, the spleen has limited capacity to support plasma cell persistence, regardless of whether they are plasmablasts or GC-derived progeny (8), and excess plasma cells generated in the immune response are lost during a contraction phase until a plateau is reached (47, 50).

As Bim-deficient AFCs gain a long-life span (17), it is conceivable that accumulation of early AFCs in the spleen for a long period may limit the subsequent recruitment of GC-derived high-affinity clones at later time points after immunization because of the inability of these cells to gain access to the relevant physical niches occupied by long-lived splenic plasma cells. Therefore, it appears that Bim plays a role in switching the antibody repertoire along the time course of the response, from the acute phase, giving rise to unmutated extrafollicular cells that are important for early protection from microbial infections, to the late phase, when high quality plasma cells participating in immune surveillance with a longer lifespan are established. The same analogy may be true for the memory B-cell responses; the early phases are low affinity with recognition of cross reactive antigens (42), but then these cells are gradually replaced by high-affinity and long-lived memory cells (26, 51), although we do not know yet whether Bim has any role in this replacement.

Bim-mediated apoptosis shortens the lifespan of unmutated extrafollicular blasts, but not of GC-derived plasma cells. BCR ligation results in interaction of Bim with Bcl-2, inhibiting its survival function (16). B cell-activating factor belonging to the tumor necrosis factor family (BAFF) and a proliferation-inducing ligand (APRIL) block BCR-induced apoptosis by downregulating Bim expression (52). The B cell maturation antigen (BCMA) binds these two ligands (BAFF and APRIL), and a homologous receptor, TACI, similarly binds both ligands [reviewed by Bossen and Schneider (53)]. BCMA deletion causes a profound loss of BM plasma cells, but no defects in short-term antibody production (54). Furthermore, it has been reported that signaling through BCMA promotes transcription of *Mcl1,* an anti-apoptotic Bcl-2 family member whose expression in BM plasma cells is crucial for their survival (55). Taken together, these results suggest that induction

of Bim-mediated apoptosis in GC-derived plasma cells is suppressed by signaling through BCMA, but that this does not occur in extrafollicular plasmablasts independent of the GC response.

Bim-mediated apoptosis affects the response by extrafollicular blasts in a T cell-dependent response, but not in the response to the T-independent (TI) type 2 antigen, NP-Ficoll. It has been observed that TACI provides an essential costimulatory signal for the T-independent humoral response (56). TACI knockouts have normal B-cell development but are deficient in their ability to mount antibody responses to TI-2 antigens (56, 57). Therefore, it is conceivable that a TACI-mediated signal suppresses Bim-mediated apoptosis in B cells in response to NP-Ficoll, but not in B cells responding to T cell-dependent antigens. Together, BCMA and TACI may play a role in inhibiting Bim-mediated apoptosis in GC-derived plasma cells and extrafollicular blasts in T cell-independent responses, respectively, but the same mechanism is not operative in extrafollicular blasts generated in T-dependent responses prior to GC formation.

GC-independent and -dependent B-cell responses develop with help from different types of T cells (26, 58–60). Bcl-6^{+}/PD-1^{hi}/CXCR5^{+} T follicular helper cells (Tfh cells) localize in follicles in the spleen where they promote GC formation and affinity maturation of B cells (61). It has been reported that Bcl-6^{+} T cells appear at the T–B border soon after T cell priming and before GC formation and that these cells express low levels of PD-1. The absence of T cells expressing Bcl-6 significantly reduces T-dependent extrafollicular antibody responses, suggesting that Bcl-6^{+} T cells are necessary at B cell priming to generate these responses (59). It remains to be elucidated how B cells acquire different properties upon stimulation with either Bcl6^{+} Tfh or non-Tfh cells in terms of susceptibility to Bim-mediated apoptosis.

It has been previously reported that deficiency of EAF2, a transcription elongation-associated factor, decreased GC B-cell apoptosis and resulted in a marginal increase in serum IgG antibodies in response to NP-CGG and NP-Ficoll (62). In contrast to Bim-deficient mice, the response was not dominated by low-affinity cells as defined by VH gene sequencing. EAF2 is involved in FAS-mediated apoptosis and EAF2 deficiency did not affect the expression of Bim (62); thus, its deficiency resulted in a different phenotype from that seen in Bim deficiency. However, Bim, EAF2 and Fas all inhibit the generation of autoantibodies, including polyreactive and anti-dsDNA antibodies, as a result of somatic mutations (16, 62–64), indicating that the maintenance of immune balance in antibody responses is regulated by multiple signaling pathways.

Data accession

Complete sequence data are available from the DNA Data Bank of Japan (DDBJ), the EMBL Nucleotide Sequence Database, and GenBank under the following accession nos.: NP-specific AFC (day 14) form *Bim*$^{+/+}$ or *Bim*$^{f/f}$ mice heterozygous for *mb-1*-cre (Fig. 4A) (Accession No. LC523040–LC523173); GC B cell separated into CD83^{high}/MHC Class II (MHC II)^{high}, CD83^{negative}/MHC II^{high} and MHC II^{dull} subsets from *Bim*$^{+/+}$ or *Bim*$^{f/f}$ mice heterozygous for *mb-1*-cre (Fig. 4B) (Accession No. LC523268–LC523528).

Funding

This work was supported by the Ministry of Education, Culture, Sports, Science, and Technology in Japan (JP19K17656) to Y.A.; AMED (JP19fk 0108051) to Y.T. and the Ministry of Education, Culture, Sports, Science and Technology in Japan (19K07618) to Ma.H.; and Riken (100266-201801022036) to Ta.T.

Acknowledgements

We appreciate Klaus Rajewsky for review and critical comments during the preparation of the manuscript. We also appreciate Tomohiro Kaji for the technical support to establish Bim cKO mice.

Author contributions

A.S.-I. and Ma.H. were responsible for established conditional *Bim* KO mice in 2015. A.S.-I. established Bim/Bcl6 double KO mice, performed experiments, data presentation and revised the manuscript. M.H. reviewed the data, prepared the manuscript and discussion. M.T. performed immunohistochemical analysis and discussion. Tom.T. informed and discussed us with his unpublished data. Y.A. and Y.T. performed influenza virus experiments. Ta.T. provided critical support. P.D.B. was responsible for discussion and critical review and edited the manuscript. Ma.H. supervised A.S.-I., discussed with Tos.T. and edited the manuscript. Tos.T. organized and designed this project and wrote the manuscript. All authors reviewed and approved the manuscript.

Conflicts of interest statement: the authors declared no conflicts of interest.

References

1 Coffey, F., Alabyev, B. and Manser, T. 2009. Initial clonal expansion of germinal center B cells takes place at the perimeter of follicles. *Immunity* 30:599.
2 Pereira, J. P., Kelly, L. M., Xu, Y. and Cyster, J. G. 2009. EBI2 mediates B cell segregation between the outer and centre follicle. *Nature* 460:1122.
3 MacLennan, I. C., Toellner, K. M., Cunningham, A. F. *et al.* 2003. Extrafollicular antibody responses. *Immunol. Rev.* 194:8.
4 Jacob, J. and Kelsoe, G. 1992. In situ studies of the primary immune response to (4-hydroxy-3-nitrophenyl)acetyl. II. A common clonal origin for periarteriolar lymphoid sheath-associated foci and germinal centers. *J. Exp. Med.* 176:679.
5 McHeyzer-Williams, M. G., McLean, M. J., Lalor, P. A. and Nossal, G. J. 1993. Antigen-driven B cell differentiation in vivo. *J. Exp. Med.* 178:295.
6 Luther, S. A., Maillard, I., Luthi, F., Scarpellino, L., Diggelmann, H. and Acha-Orbea, H. 1997. Early neutralizing antibody response against mouse mammary tumor virus: critical role of viral infection and superantigen-reactive T cells. *J. Immunol.* 159:2807.
7 Zhang, Y., Meyer-Hermann, M., George, L. A. *et al.* 2013. Germinal center B cells govern their own fate via antibody feedback. *J. Exp. Med.* 210:457.
8 Sze, D. M., Toellner, K. M., García de Vinuesa, C., Taylor, D. R. and MacLennan, I. C. 2000. Intrinsic constraint on plasmablast growth and extrinsic limits of plasma cell survival. *J. Exp. Med.* 192:813.
9 Smith, K. G., Light, A., Nossal, G. J. and Tarlinton, D. M. 1997. The extent of affinity maturation differs between the memory and antibody-forming cell compartments in the primary immune response. *EMBO J.* 16:2996.
10 Takahashi, Y., Dutta, P. R., Cerasoli, D. M. and Kelsoe, G. 1998. In situ studies of the primary immune response to (4-hydroxy-3-nitrophenyl)acetyl. V. Affinity maturation develops in two stages of clonal selection. *J. Exp. Med.* 187:885.
11 Weisel, F. J., Zuccarino-Catania, G. V., Chikina, M. and Shlomchik, M. J. 2016. A temporal switch in the germinal center determines differential output of memory B and plasma cells. *Immunity* 44:116.

12 Slifka, M. K., Antia, R., Whitmire, J. K. and Ahmed, R. 1998. Humoral immunity due to long-lived plasma cells. *Immunity* 8:363.
13 Slifka, M. K., Matloubian, M. and Ahmed, R. 1995. Bone marrow is a major site of long-term antibody production after acute viral infection. *J. Virol.* 69:1895.
14 Marsden, V. S. and Strasser, A. 2003. Control of apoptosis in the immune system: Bcl-2, BH3-only proteins and more. *Annu. Rev. Immunol.* 21:71.
15 Youle, R. J. and Strasser, A. 2008. The BCL-2 protein family: opposing activities that mediate cell death. *Nat. Rev. Mol. Cell Biol.* 9:47.
16 Enders, A., Bouillet, P., Puthalakath, H., Xu, Y., Tarlinton, D. M. and Strasser, A. 2003. Loss of the pro-apoptotic BH3-only Bcl-2 family member Bim inhibits BCR stimulation-induced apoptosis and deletion of autoreactive B cells. *J. Exp. Med.* 198:1119.
17 Fischer, S. F., Bouillet, P., O'Donnell, K., Light, A., Tarlinton, D. M. and Strasser, A. 2007. Proapoptotic BH3-only protein Bim is essential for developmentally programmed death of germinal center-derived memory B cells and antibody-forming cells. *Blood* 110:3978.
18 O'Reilly, L. A., Cullen, L., Visvader, J. *et al.* 2000. The proapoptotic BH3-only protein bim is expressed in hematopoietic, epithelial, neuronal, and germ cells. *Am. J. Pathol.* 157:449.
19 Chen, M., Huang, L. and Wang, J. 2007. Deficiency of Bim in dendritic cells contributes to overactivation of lymphocytes and autoimmunity. *Blood* 109:4360.
20 Andina, N., Conus, S., Schneider, E. M., Fey, M. F. and Simon, H. U. 2009. Induction of Bim limits cytokine-mediated prolonged survival of neutrophils. *Cell Death Differ.* 16:1248.
21 Zhan, Y., Zhang, Y., Gray, D. *et al.* 2011. Defects in the Bcl-2-regulated apoptotic pathway lead to preferential increase of CD25 low Foxp3+ anergic CD4+ T cells. *J. Immunol.* 187:1566.
22 Chougnet, C. A., Tripathi, P., Lages, C. S. *et al.* 2011. A major role for Bim in regulatory T cell homeostasis. *J. Immunol.* 186:156.
23 Wang, X., Szymczak-Workman, A. L., Gravano, D. M., Workman, C. J., Green, D. R. and Vignali, D. A. 2012. Preferential control of induced regulatory T cell homeostasis via a Bim/Bcl-2 axis. *Cell Death Dis.* 3:e270.
24 Casola, S., Cattoretti, G., Uyttersprot, N., Koralov, S. B., Seagal, J., Hao, Z., Waisman, A., Egert, A., Ghitza, D. and Rajewsky, K. 2006. Tracking germinal center B cells expressing germ-line immunoglobulin γ1 transcripts by conditional gene targeting. *Proc. Natl Acad. Sci. USA.* 103:7396.
25 Hobeika, E., Thiemann, S., Storch, B. *et al.* 2006. Testing gene function early in the B cell lineage in mb1-cre mice. *Proc. Natl Acad. Sci. USA.* 103:13789.
26 Kaji, T., Ishige, A., Hikida, M. *et al.* 2012. Distinct cellular pathways select germline-encoded and somatically mutated antibodies into immunological memory. *J. Exp. Med.* 209:2079.
27 Takahashi, Y., Ohta, H. and Takemori, T. 2001. Fas is required for clonal selection in germinal centers and the subsequent establishment of the memory B cell repertoire. *Immunity* 14:181.
28 Köntgen, F., Süss, G., Stewart, C., Steinmetz, M. and Bluethmann, H. 1993. Targeted disruption of the MHC class II Aa gene in C57BL/6 mice. *Int. Immunol.* 5:957.
29 Kanki, H., Suzuki, H. and Itohara, S. 2006. High-efficiency CAG-FLPe deleter mice in C57BL/6J background. *Exp. Anim.* 55:137.
30 Allman, D., Lindsley, R. C., DeMuth, W., Rudd, K., Shinton, S. A. and Hardy, R. R. 2001. Resolution of three nonproliferative immature splenic B cell subsets reveals multiple selection points during peripheral B cell maturation. *J. Immunol.* 167:6834.
31 Nagaoka, H., Takahashi, Y., Hayashi, R. *et al.* 2000. Ras mediates effector pathways responsible for pre-B cell survival, which is essential for the developmental progression to the late pre-B cell stage. *J. Exp. Med.* 192:171.
32 Adachi, Y., Tonouchi, K., Nithichanon, A. *et al.* 2019. Exposure of an occluded hemagglutinin epitope drives selection of a class of cross-protective influenza antibodies. *Nat. Commun.* 10:3883.
33 Kaji, T., Hijikata, A., Ishige, A. *et al.* 2016. CD4 memory T cells develop and acquire functional competence by sequential cognate interactions and stepwise gene regulation. *Int. Immunol.* 28:267.
34 Sionov, R. V., Vlahopoulos, S. A. and Granot, Z. 2015. Regulation of Bim in health and disease. *Oncotarget* 6:23058.
35 Bouillet, P., Metcalf, D., Huang, D. C. *et al.* 1999. Proapoptotic Bcl-2 relative Bim required for certain apoptotic responses, leukocyte homeostasis, and to preclude autoimmunity. *Science* 286:1735.
36 O'Connor, L., Strasser, A., O'Reilly, L. A. *et al.* 1998. Bim: a novel member of the Bcl-2 family that promotes apoptosis. *EMBO J.* 17:384.
37 Oliver, P. M., Wang, M., Zhu, Y., White, J., Kappler, J. and Marrack, P. 2004. Loss of Bim allows precursor B cell survival but not precursor B cell differentiation in the absence of interleukin 7. *J. Exp. Med.* 200:1179.
38 Liu, R., King, A., Bouillet, P., Tarlinton, D. M., Strasser, A. and Heierhorst, J. 2018. Proapoptotic BIM impacts B lymphoid homeostasis by limiting the survival of mature B cells in a cell-autonomous manner. *Front. Immunol.* 9:592.
39 Craxton, A., Draves, K. E. and Clark, E. A. 2007. Bim regulates BCR-induced entry of B cells into the cell cycle. *Eur. J. Immunol.* 37:2715.
40 Gao, Y., Kazama, H. and Yonehara, S. 2012. Bim regulates B-cell receptor-mediated apoptosis in the presence of CD40 signaling in CD40-pre-activated splenic B cells differentiating into plasma cells. *Int. Immunol.* 24:283.
41 Allen, D., Simon, T., Sablitzky, F., Rajewsky, K. and Cumano, A. 1988. Antibody engineering for the analysis of affinity maturation of an anti-hapten response. *EMBO J.* 7:1995.
42 Kaji, T., Furukawa, K., Ishige, A. *et al.* 2013. Both mutated and unmutated memory B cells accumulate mutations in the course of the secondary response and develop a new antibody repertoire optimally adapted to the secondary stimulus. *Int. Immunol.* 25:683.
43 Victora, G. D., Dominguez-Sola, D., Holmes, A. B., Deroubaix, S., Dalla-Favera, R. and Nussenzweig, M. C. 2012. Identification of human germinal center light and dark zone cells and their relationship to human B-cell lymphomas. *Blood* 120:2240.
44 Bannard, O., McGowan, S. J., Ersching, J. *et al.* 2016. Ubiquitin-mediated fluctuations in MHC class II facilitate efficient germinal center B cell responses. *J. Exp. Med.* 213:993.
45 Lu, Y. F., Singh, M. and Cerny, J. 2001. Canonical germinal center B cells may not dominate the memory response to antigenic challenge. *Int. Immunol.* 13:643.
46 Furukawa, K., Akasako-Furukawa, A., Shirai, H., Nakamura, H. and Azuma, T. 1999. Junctional amino acids determine the maturation pathway of an antibody. *Immunity* 11:329.
47 Manz, R. A., Thiel, A. and Radbruch, A. 1997. Lifetime of plasma cells in the bone marrow. *Nature* 388:133.
48 Ellyard, J. I., Avery, D. T., Phan, T. G., Hare, N. J., Hodgkin, P. D. and Tangye, S. G. 2004. Antigen-selected, immunoglobulin-secreting cells persist in human spleen and bone marrow. *Blood* 103:3805.
49 Wilmore, J. R. and Allman, D. 2017. Here, there, and anywhere? Arguments for and against the physical plasma cell survival niche. *J. Immunol.* 199:839.
50 Kallies, A., Hasbold, J., Tarlinton, D. M. *et al.* 2004. Plasma cell ontogeny defined by quantitative changes in blimp-1 expression. *J. Exp. Med.* 200:967.
51 Weisel, F. and Shlomchik, M. 2017. Memory B cells of mice and humans. *Annu. Rev. Immunol.* 35:255.
52 Craxton, A., Draves, K. E., Gruppi, A. and Clark, E. A. 2005. BAFF regulates B cell survival by downregulating the BH3-only family member Bim via the ERK pathway. *J. Exp. Med.* 202:1363.
53 Bossen, C. and Schneider, P. 2006. BAFF, APRIL and their receptors: structure, function and signaling. *Semin. Immunol.* 18:263.
54 O'Connor, B. P., Raman, V. S., Erickson, L. D. *et al.* 2004. BCMA is essential for the survival of long-lived bone marrow plasma cells. *J. Exp. Med.* 199:91.
55 Peperzak, V., Vikström, I., Walker, J. *et al.* 2013. Mcl-1 is essential for the survival of plasma cells. *Nat. Immunol.* 14:290.
56 von Bülow, G. U., van Deursen, J. M. and Bram, R. J. 2001. Regulation of the T-independent humoral response by TACI. *Immunity* 14:573.
57 Yan, M., Wang, H., Chan, B. *et al.* 2001. Activation and accumulation of B cells in TACI-deficient mice. *Nat. Immunol.* 2:638.

58 Taylor, J. J., Pape, K. A. and Jenkins, M. K. 2012. A germinal center-independent pathway generates unswitched memory B cells early in the primary response. *J. Exp. Med.* 209:597.
59 Lee, S. K., Rigby, R. J., Zotos, D. *et al.* 2011. B cell priming for extrafollicular antibody responses requires Bcl-6 expression by T cells. *J. Exp. Med.* 208:1377.
60 Linterman, M. A., Pierson, W., Lee, S. K. *et al.* 2011. Foxp3^{+} follicular regulatory T cells control the germinal center response. *Nat. Med.* 17:975.
61 Crotty, S. 2019. T follicular helper cell biology: a decade of discovery and diseases. *Immunity* 50:1132.
62 Li, Y., Takahashi, Y., Fujii, S. *et al.* 2016. EAF2 mediates germinal centre B-cell apoptosis to suppress excessive immune responses and prevent autoimmunity. *Nat. Commun.* 7:10836.
63 Hughes, P. D., Belz, G. T., Fortner, K. A., Budd, R. C., Strasser, A. and Bouillet, P. 2008. Apoptosis regulators Fas and Bim cooperate in shutdown of chronic immune responses and prevention of autoimmunity. *Immunity* 28:197.
64 Tiller, T., Kofer, J., Kreschel, C. *et al.* 2010. Development of self-reactive germinal center B cells and plasma cells in autoimmune Fc gammaRIIB-deficient mice. *J. Exp. Med.* 207:2767.